Report No. 98

The Institute of Hydrology Distributed Model

K. Beven, A. Calver and E.M. Morris

December 1987

Contents

Abstract

This report describes the Institute of Hydrology Distributed Model, a physically-based catchment model for overland flow, saturated and unsaturated subsurface flow and channel flow.

The history of the model's development is outlined and subsequent attention is focussed on the most recent version, the IHDM4.

The concepts of catchment representation and overall model structure are discussed. Detail is then provided on the individual model subroutines, covering the finite diffference overland and channel flow solution and the finite element subsurface solution.

Example runoff simulations are presented. Calibration and validation procedures are discussed in the context of the use of such distributed models.

1. Introduction

The original stimulus for the development of physically-based catchment models at the Institute of Hydrology came from a desire to make flood forecasts on ungauged catchments and predict the hydrological effects of land use change. There was a particular desire to model the differing responses of the Institute's Wye and Severn experimental catchments at Plynlimon which differ primarily in vegetation cover but also to some extent in topography, channel network geometry and soils. Once the techniques had been proven on the Plynlimon catchments it was intended to predict the hydrological response and the effects of land use change on other upland catchments, since the physical basis of this type of model allows either direct measurement of parameters or estimation on the basis of physical characteristics of a catchment. Work on the Institute of Hydrology Distributed Model, IHDM, has been funded since its inception by the Ministry of Agriculture, Fisheries and Food, UK.

An early discussion of the possibility of a physically-based model of catchment hydrology was that of Freeze and Harlan (1969), who described the necessary assumptions and flow equations required. The application of such a model to limited hypothetical problems using finite difference methods to solve the partial differential equations of flow was demonstrated by Freeze (1971, 1972a, b). Other catchment scale physically-based models of differing degrees of complexity have been published by Smith and Woolhiser (1971), Engman and Rogowski (1974) and Ross et al. (1979) while there have been many other studies of individual process components. The advantages of such models are that they are based directly on descriptions of processes observed in the field and have parameters that are directly measureable. More detailed discussions of the rationale and problems of physically-based modelling may be found in Freeze (1978), Beven and O'Connell (1982) and Beven (1985).

The Institute has been involved in the development of two catchment scale physically-based models since 1977. The Système Hydrologique Européen (SHE) model was a joint project with the Danish Hydraulics Institute (DHI) and SOGREAH of France. The structure of the SHE model is described in Beven et al. (1980) and Abbott et al. (1986a, b). The SHE model uses a fixed square grid in its spatial discretisation of a catchment area and while it is well suited to modelling catchments with important groundwater systems or widespread infiltration excess overland flow, its fixed grid creates a limit on the resolution with which it can represent the spread of areas of saturation and surface flow close to channels. Such areas may be strongly dependent on topographic convergence and divergence which may not be well represented with a square grid except by using very small grid elements, which would result in computations involving very large matrices. It should be noted however that Bathurst (1986) has recently reported successful simulations of the Wye catchment response using the SHE model and a grid scale of 250 m square. The alternative structure of the IHDM has continued to be explored since it allows much finer definition at the bottom of hillslopes and can predict two-dimensional flows in the unsaturated zone. It was expected that the IHDM would be a suitable structure for use in upland catchments, while the SHE model may be more appropriate in areas with a strong regional groundwater component.

2. Development of the IHDM

The first version of the IHDM was written in 1977 and combined a finite difference solution of the one-dimensional Saint-Venant equations for overland and channel flows with a conceptual soil water storage model. The basic structure of the IHDM which involves the sequential solution of a network of hillslope and channel components (figure 1) was formulated at this time. The catchment is divided into hillslope planes along lines of greatest slope orthogonal to the contours. No-flow boundaries are assumed to exist between adjacent hillslope planes. Each hillslope plane represents the whole length of a hillslope (ie. a plane cannot cascade into a lower hillslope plane) and contributes lateral or headwater discharge into a channel component at its base. In version 1 of the IHDM the hillslope planes were treated as rectangles of length and slope angle representative of the real topography. Overland flow was generated over the whole length of the hillslope plane whenever the soil moisture storage deficit was satisfied by the storm inputs (figure 2a). The channel components were also of constant slope and rectangular cross-section. Results using this model were reported in Morris (1980).

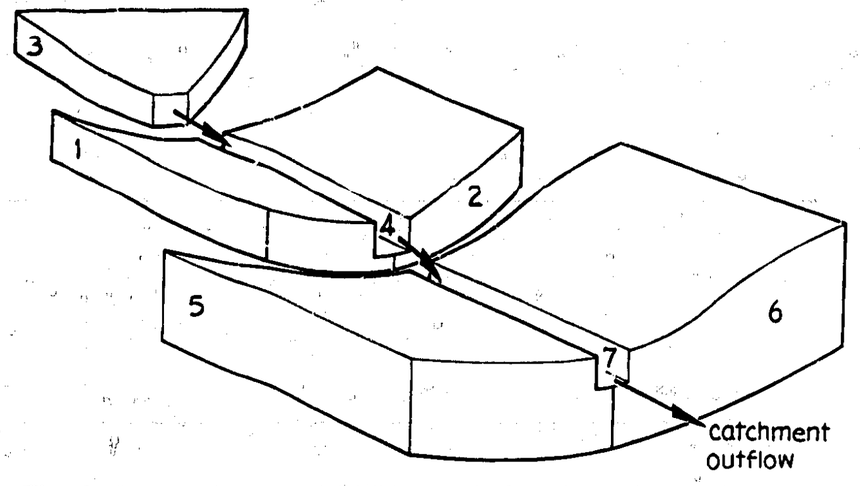

Fig. 1 Schematic structure of hillslope and channel components of the IHDM. 1, 2, 5, 6 hillslope component (sideslope); 3 hillslope component (headwater); 4, 7 channel component. Numbering indicates order of simulation of components.

In version 2 of the model the conceptual soil water storage was replaced by a two-dimensional, vertical cross-section, finite difference solution of the Richards equation for flow in partially saturated soil on each hillslope plane. The planes remained rectangular in form. The solution used an efficient predictor-corrector finite difference scheme using only tridiagonal matrices based on a regular grid in which the vertical and horizontal nodal spacings were controlled by the slope angle (figure 2b). This version of the model is described in Morris et al. (1980). Later modifications were made that allowed the area of overland flow on a hillslope plane to expand and contract dynamically.

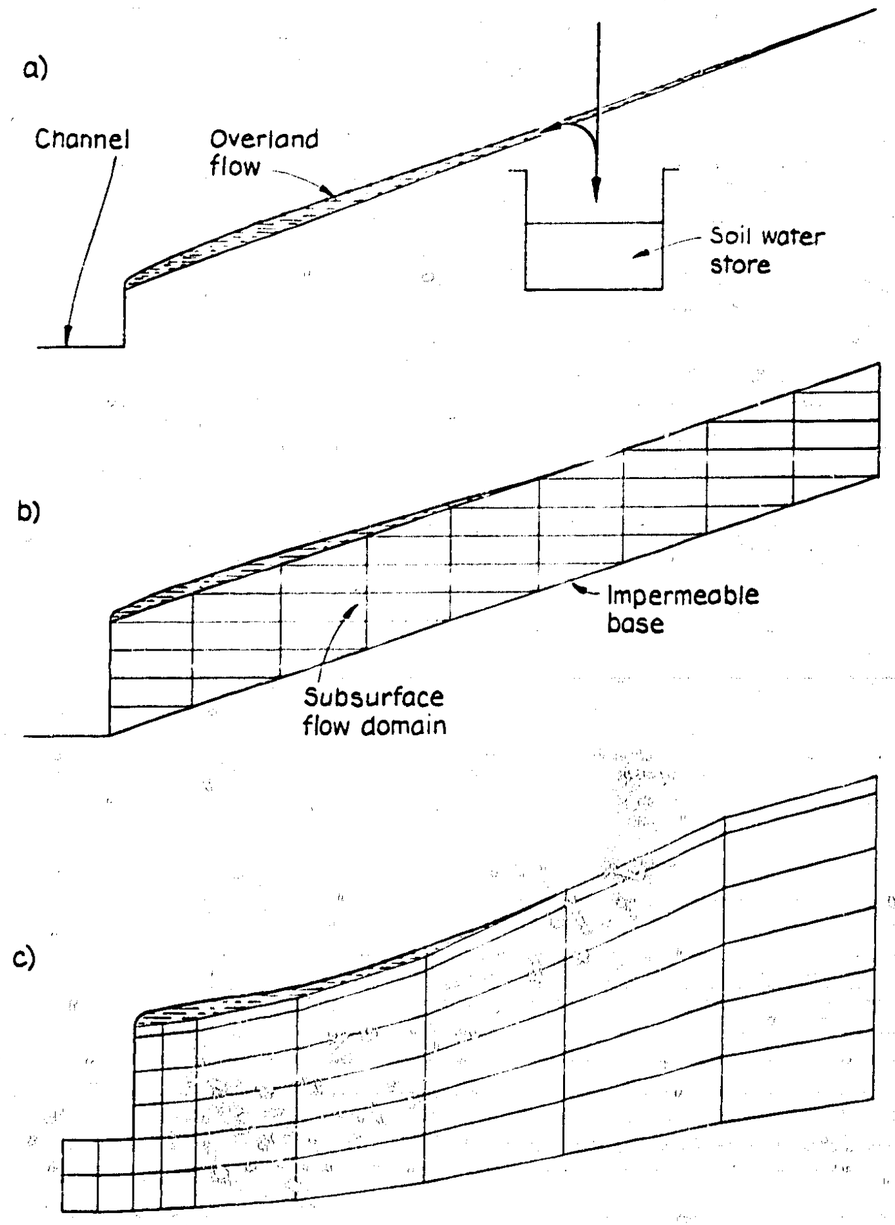

Fig. 2 Diagrammatic structure of IHDM hillslopes
a) version 1
b) versions 2 and 3
c) version 4

Further development of the model resulted in version 3 which had much more flexible routines controlling evapotranspiration from surface water and the root zone. Interception and snowmelt calculations were also incorporated into a preprogram that calculates throughfall, stemflow, melt and evapotranspiration fluxes at the ground surface for use by the hydrological model for each of a number of input zones (see section 3). The subsurface solution remained essentially the same as the preceding version, but alternative overland and channel flow solutions based on the kinematic wave equation were incorporated for use in steep channels where any backwater and dynamic wave effects could be neglected (see for example Morris and Woolhiser, 1980).

The subsurface flow solution of version 3 proved to be a limitation on the application of the model since with certain combinations of parameter values, time steps and input sequences the solution would not remain stable. Consequently, it was decided to rewrite the hillslope component completely, at the same time making the representation of hillslopes much more flexible. The resulting version 4 of the model is the main subject of this report. The hillslope planes now use a finite element solution of the Richards equation which allows the planes to vary in width to take account of hillslope flow convergence, in depth to allow deeper soils to be modelled and to have several different soil horizons of differing soil hydraulic properties (figure 2c). Automatic program control of time steps has also been added. The new solution scheme has proved to be numerically well-behaved under a variety of conditions for which tests have been carried out. Version 4 of the model has been implemented on IBM PC and Research Machines Nimbus micro-computers in addition to mainframe computers.

3. The calculation of model inputs

3.1 The concept of input zones

The calculation of the input fluxes at ground level to the model may be carried out in a separate preprogram, GLI, prior to the use of the IHDM itself. Alternatively, observed or calculated effective precipitation values may be input directly. The GLI program is structured so that separate calculations may be made for a number of different input zones. These zones may differ in meteorological inputs, elevation range, slope angle, aspect, and vegetation type (figure 3), all of which affect the interception, snowmelt and evapotranspiration calculations outlined in section 3.2.

Within the IHDM each finite element boundary segment on the surface of a hillslope plane is associated with a particular zone with its own sequence of inputs. This allows very flexible but also efficient handling of spatially variable inputs to the hydrological model. Each hillslope plane may have an arbitrary number of zonal inputs within the limits set by the array bounds in the program (currently 12 zones). Any zone, however, may cover all or parts of more than one hillslope plane where the zonal characteristics are common.

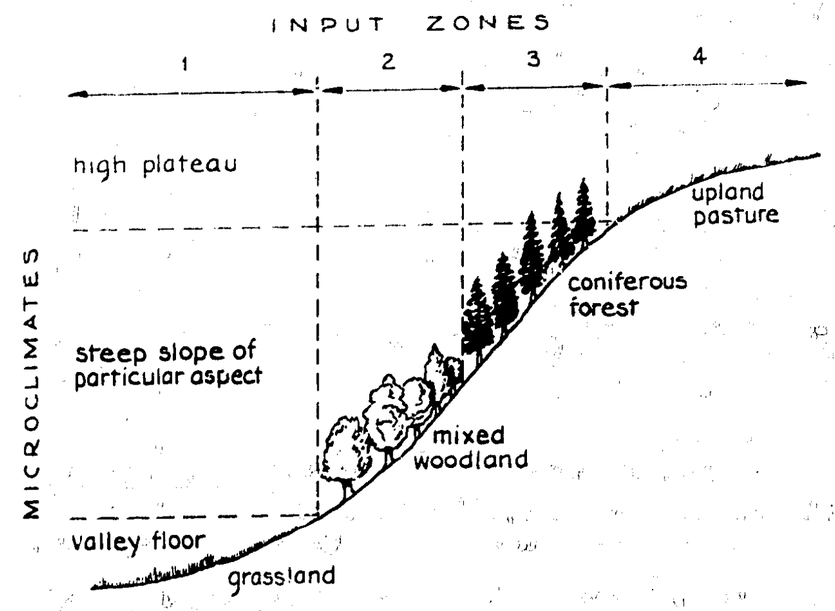

Fig. 3 Schematic representation of model input zones.

The hillslopes or parts of hillslopes within a particular zone need not be spatially contiguous. This has proved particularly useful in modelling responses during snowmelt periods where hillslopes with similar elevation, aspect and slope angle characteristics could be included within a single zone (see figure 4).

The ground level fluxes output by the GLI program may be either positive or negative. A negative surface flux indicates that there is some residual potential evapotranspiration to be distributed between the surface and the root zone. Reductions in actual evapotranspiration in the root zone are dependent on local values of capillary potential (see section 4.2.4).

3.2 Preprograms MET and GLI

Program MET is designed to produce meteorological input data for various zones in a catchment by making adjustments to measured data from a meteorological station, which may or may not be within the catchment. Each model zone is characterised by altitude and orientation by classifying it as of a certain elevation zone type and radiation zone type. At the moment the program uses either hourly data from a base automatic weather station, a standard Institute of Hydrology AWS or a 'Super' IH AWS.

In preprogram GLI the corrected meteorological data for each zone of a catchment are used to calculate interception and evapotranspiration or snowmelt for that zone. The meteorological data are further adjusted for the effect of changing albedo and differences in vegetation. If measured net

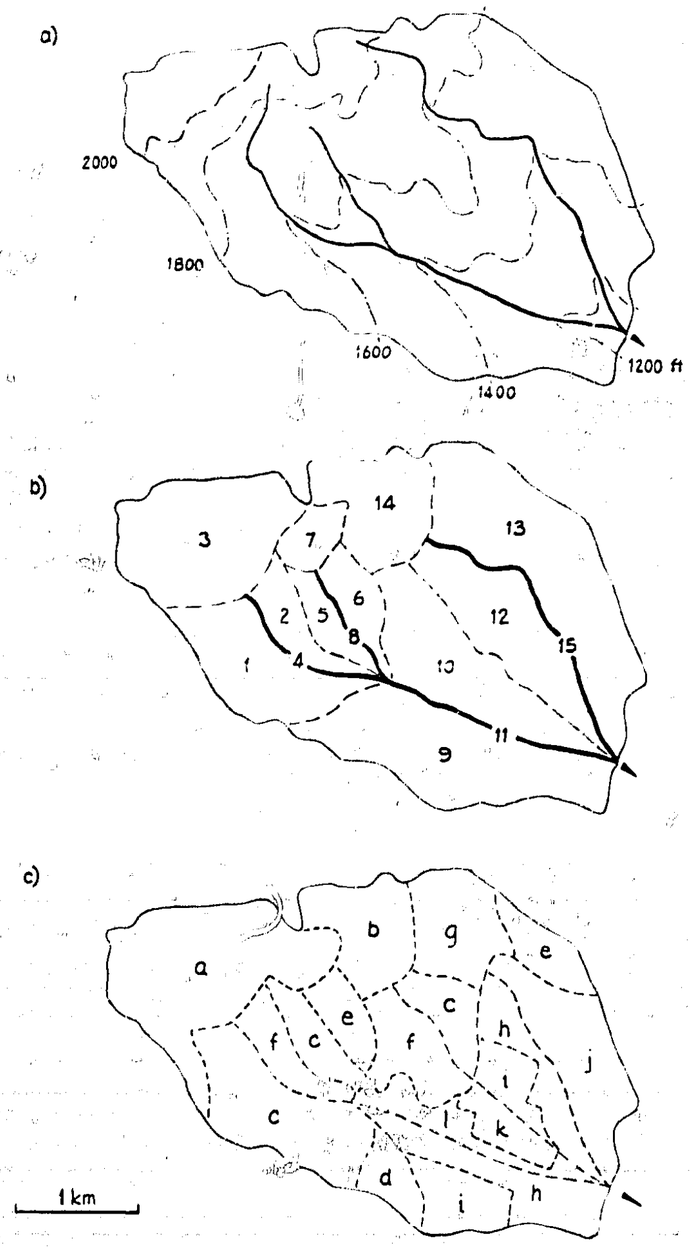

Fig. 4 Spatial division of a catchment for model use, Vermont USA
a) channels and contours
b) hillslope and channel divisions
c) surface zones for input calculations

radiation data are not available they are estimated by calculating net longwave and shortwave radiation separately. If snowmelt is to be calculated there is a choice of two methods, an energy budget method and a temperature index method. For cases of no snow cover, potential evapotranspiration is calculated from a Penman-Monteith equation. Evaporation of intercepted water from a wet canopy is calculated with reference to vegetation cover characteristics, changes in canopy storage being predicted using a modified form of the Rutter model. The output from the program is the ground level input of effective rainfall or meltwater for each zone which is required as input for the main program of the IHDM.

Preprograms MET and GLI have been tested at two snow sites: on the Hardanger Plateau in southern Norway and on the Hintereis glacier in the Austrian Alps. In both cases it was shown that the changes in the snow depths could be predicted provided the aerodynamic roughness lengths of the snow were known.

4. Description of the IHDM program

4.1. General outline : the CONTROL routine

The network or cascade structure of the IHDM has facilitated a modular programming approach to the model. A formal flow diagram of the subroutine structure of the model is shown in figure 5. Subroutine CONTROL directs the overall operation of the model, assembling catchment data, carrying out hillslope and channel calculations as appropirate, tallying transfers between components and calculating catchment water balance.

4.1.1 Network definition in the IHDM

The network of hillslope and channel components for a particular catchment is defined by an array of integer values, with one value for each component. The user, in defining the values of the array, specifies the order of calculation of the various hillslope and channel components making up the model of the catchment. Care must therefore be taken to ensure that when the calculations for a given component are started discharges from all components higher in the network (in an elevation sense) are available. It is useful in this respect to order the channel calculations first, later adding the hillslope planes contributing to each channel.

The channel sections in a network may be classified into four types which are given different integer numbers in the network definition array. Type 3 refers to the first channel above a junction in terms of calculation order: type 4 refers to the second channel above a junction. Type 5 indicates that the channel discharges should be stored pending completion of the calculations in a different arm of the network. Type 6 indicates a channel that has a downstream junction with a channel of type 5. Figure 6a demonstrates the classification of a simple channel network according to these types.

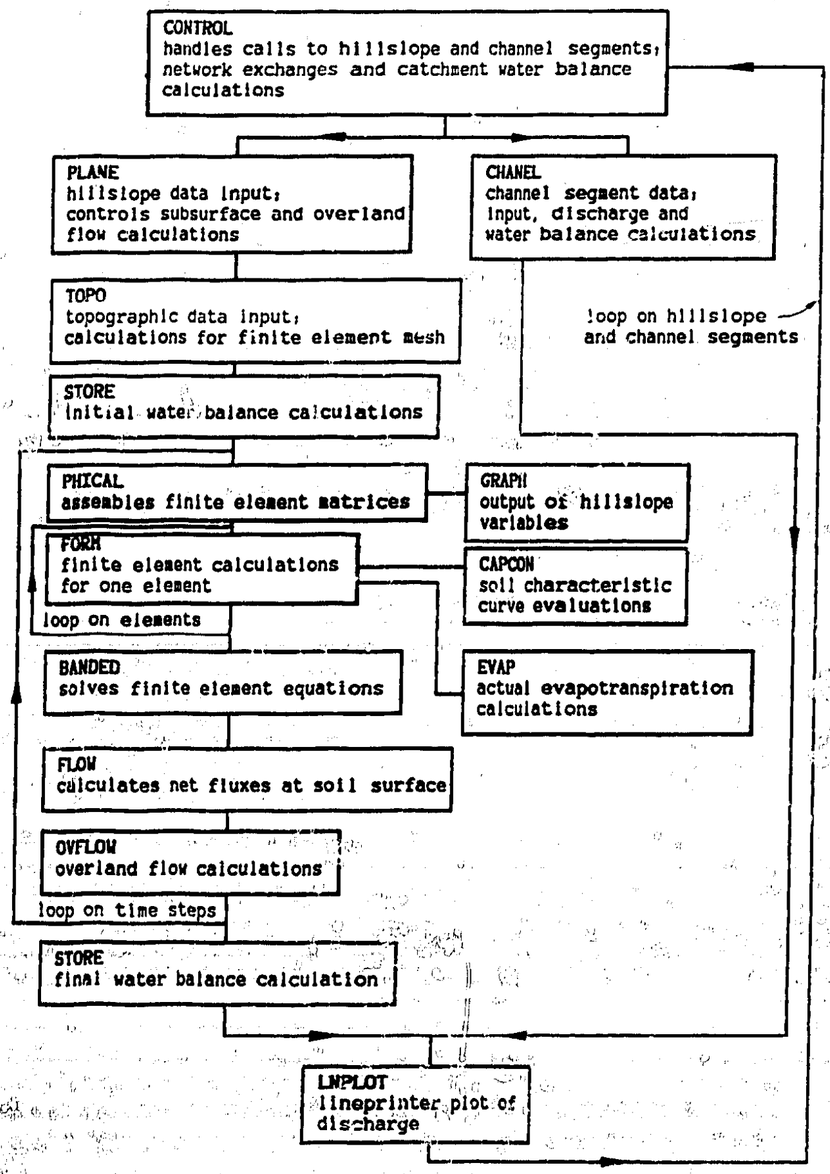

Fig. 5 Flow diagram of IHDM programming structure

The hillslope planes in a network may be classified into two types. Type 1 refers to a sideslope plane which contributes discharge laterally into a channel section. Type 2 indicates a headwater plane which contributes discharge into

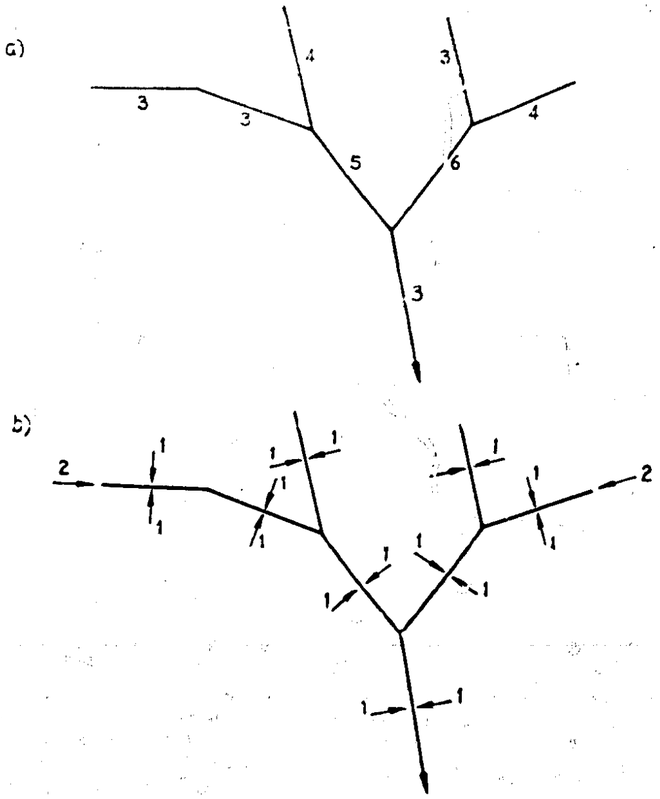

Fig. 6 Classifcation of a) channel types and b) hillslope types in a network

the head of a first order channel. Figure 6b shows a classification of the hillslope planes for the simple network according to these types. A final network definition array for this catchment system could be specified as
1 1 2 3 1 1 3 1 1 4 1 1 5 1 1 3 1 1 2 4 1 1 6 1 1 3
(though it will be apparent that there are other appropriate orderings).

4.1.2 Time steps in the IHDM

There are four levels of time step in version 4 of the IHDM. The highest level is the input data time step, which is controlled by the outputs available from the GLI preprogram. In the applications carried out to date this time step has been typically one hour. The next level is the time step used for exchanging fluxes between the hillslope and channel components. This level also defines the resolution with which the final discharges predicted for the catchment will be produced. This can be equal to or smaller than the input step but there is always an integer number of 'exchange' time steps in each input time step.

The third level is the time step used in the subsurface flow and channel flow calculations. For the channels there is an integer number of time steps in each exchange time step, but the hillslope calculation time step is allowed to vary under program control. In either case the maximum value allowed is equal to or less than the exchange step. Finally there is the time step used in the overland flow calculations on the hillslopes. There is a fixed integer number of overland flow time steps in each subsurface flow time step.

4.2 Hillslope calculations: the PLANE routine

The flow calculations on each hillslope plane are controlled by subroutine PLANE which carries out initialisation and water balance calculations for both the subsurface and overland flow solutions. It also contains the main time step loops and the program control of the subsurface time step. The governing equations on which the solutions are based are developed as follows for the general case of a two-dimensional vertical cross-section through a variable width slope.

For the subsurface flow domain, the development of the fundamental equations of saturated/unsaturated flow in a porous medium derive from the work of Richards (1931). A detailed exposition may be found for example in Bear (1972). In the formulation used here the following assumptions are made.

a) The water is assumed to be of constant viscosity and unit density.
b) The flow is assumed to be laminar and of low velocity in an isothermal medium.
c) The flow is assumed to be adequately described by Darcy's law, with time-invariant parameters.
d) Although the medium is allowed to be anisotropic the principal axes of the hydraulic conductivity tensor are assumed to be parallel to the global x, z axes.
e) Only single phase water flow in response to hydraulic pressure gradients is considered, the effects of air and water vapour flows, temperature, osmotic gradients and other forces being neglected.

Within the limitations of these assumptions, for a slope with gradually varying width, the Richards equation may be expressed in the form:

$$B\frac{\partial\theta}{\partial t} - \frac{\partial}{\partial x}\left[B\,K_x\frac{\partial\phi}{\partial x}\right] - \frac{\partial}{\partial z}\left[B\,K_z\frac{\partial\phi}{\partial z}\right] = Q_s \qquad (1)$$

where θ is soil moisture content by volume, ψ is capillary potential, z is vertical distance measured from some arbitrary datum, $\phi = \psi + z$ is total hydraulic potential, K is the hydraulic conductivity, a non-linear function of ψ, B is slope width, x is horizontal distance downslope, Q_s is a source/sink term and t is time.

The current version of the IHDM uses a ϕ-based solution scheme, which requires a further assumption that there is a relationship between θ and ψ that is locally differentiable. The variable $C(\psi) = d\theta/d\psi$ is normally called the specific moisture capacity of the soil. Equation 1 can then be written in the form

$$B\,C(\psi)\frac{\partial\phi}{\partial t} - \frac{\partial}{\partial x}\left[B\,K_x(\psi)\frac{\partial\phi}{\partial x}\right] - \frac{\partial}{\partial z}\left[B\,K_z(\psi)\frac{\partial\phi}{\partial z}\right] = Q_s \qquad (2)$$

Equation 2 is solved by a finite element method, details of which are given below.

Subroutine PLANE also sets up the initial conditions on each hillslope. Five options are available to set up the initial values of ψ at each node. In the first the values are simply read from a file. This file can be set up by the user or can be produced by an earlier run of the model since each hillslope and channel component automatically writes the dependent variables to a file at the end of each run. The other four initial condition options are detailed in table 1. For the initial conditions other than those read from a file the fixed head nodes adjacent to the channel are initialised at the difference between the read-in fixed potential and the nodal elevation.

When surface flow occurs on the hillslope, due either to the infiltration capacity of the soil surface being exceeded by the input rates, or to the soil

TABLE 1. Subsurface flow initial condition options

PSI(I) is the initial moisture potential and Z(I) is the elevation of the Ith node

Option No	Initial Condition	Input Variables
0	Values read from file.	PSI(I)
1	PSI(I)=YIN everywhere on hillslope.	YIN
2	Water table position calculated from an initial steady state flow (XIN) which is assumed to be supplied by uniform saturated downslope flow per unit area of slope. Above the water table PSI(I)=Z – Z(I) if PSI(I) > YIN else PSI(I)=YIN, where Z is local elevation of water table.	XIN, YIN
3	PSI(I) = XIN – Z(I) if PSI(I) > YIN, else PSI(I)=YIN, where XIN is potential at base of slope	XIN,YIN
4	PSI(I) = (1–YIN)(XIN–Z(I)), XIN as in option 3	XIN,YIN

being fully saturated to the surface when there may be a return flow back to the surface even in the absence of inputs, then an overland flow solution is required. The description of overland flow is based on a kinematic wave equation for a variable width slope

$$\frac{B\partial Q}{\partial t} + c\frac{\partial}{\partial y}(BQ) - Bic = 0 \qquad (3)$$

where Q is discharge, i is net lateral inflow rate per unit downslope length, y is distance downslope and c is the kinematic wave velocity defined by dQ/dA where A is the cross-sectional area of flow. The kinematic wave description of overland flow has been used in many previous distributed models (eg. Smith and Woolhiser, 1971; Engman and Rogowski, 1974; Ross et al., 1979). Conditions under which the kinematic flow equation may be considered as an acceptable approximation to the more complete Saint-Venant equations have been considered by Woolhiser and Liggett (1967), Morris and Woolhiser (1980) and Daluz Vieira (1983).

4.2.1 The analysis of hillslope topography: the TOPO routine

Any physically-based model that uses an approximate numerical solution to the partial differential equations of flow bases its calculations on values of the variables of interest (eg. capillary potentials or channel discharges) at a large number of points or nodes in space. The greater the number of nodes, the greater the resolution with which predictions may be made. However, computer run times increase rapidly as the number of nodes increases. This problem has precluded the use of fully three-dimensional models except on somewhat limited problems. Thus any physically-based model must reach a compromise between spatial resolution and computational expense.

One way of doing this is to reduce the dimensionality of the problem. For example, in the IHDM, the subsurface solution is 'averaged' across the width of a slope so that predictions are made for a representative vertical cross-section such as that shown in figure 7. Similarly, the channels are generalised into equivalent one-dimensional representations. While the resultant 'topography' is only a broad generalisation of the real catchment, this structure has two computational advantages. The hillslope planes can simulate the essential effects of topographic convergence and slope variations without the number of solution nodes required in a fully three-dimensional representation. In addition the way that the plane calculations are carried out sequentially means computer storage requirements at any time are not excessive.

It is clear that the choice of hillslope planes is always subjective and demands continual compromise between the requirements of representing the catchment in a reasonably faithful way and the computational burden of a finer discretisation. It is felt, however, that the structure of the IHDM now allows a better representation of catchment topography than has been possible in earlier physically-based models. The limitations of the present version will be felt only in catchments where the directions of flow in the saturated zone do not conform to the surface topography, such as in some cases of a regional groundwater system: the lack of exchanges between the hillslope planes will

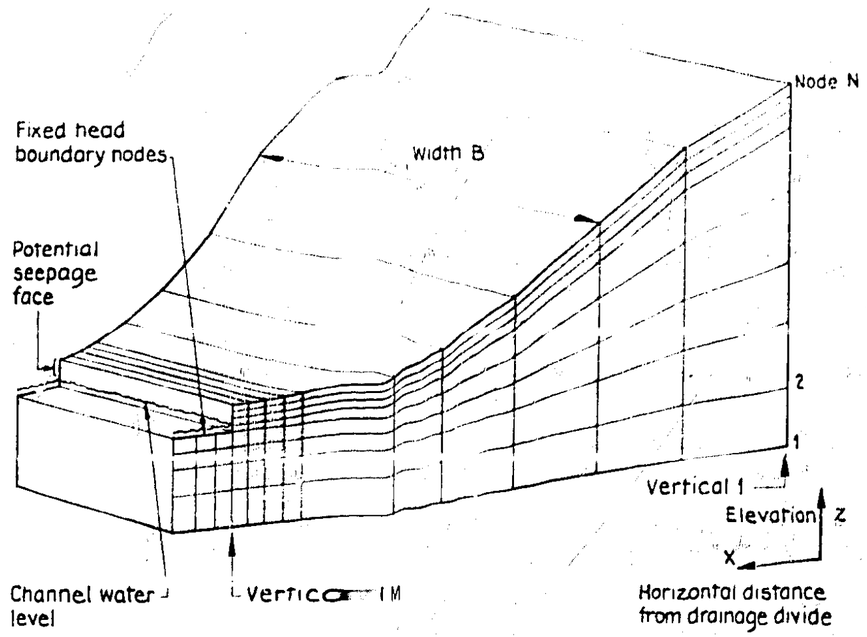

Fig. 7 Hillslope finite element mesh example

then restrict the physical basis of the predictions of the IHDM.

Definition of each hillslope plane is based on an N by M grid of solution nodes to represent the main part of the hillslope, where N is the number of nodes in each vertical line, and M is the number of vertical lines of nodes (see figure 7). For each of the M lines of nodes, a horizontal distance from the upslope boundary, a plane width, a surface elevation value and the depths of the N nodes in that line are specified. Within each vertical line of nodes it is assumed that the slope width is a constant. In addition there may be additional rectangular finite elements at the bottom of the slope which may extend under the channel (figure 7). The x, z coordinates of the nodes of these additional elements are input individually and the width of the additional elements is assumed to be the same as that of the Mth line of nodes on the main part of the slope.

The allowable boundary conditions for each hillslope plane are conditioned by the requirement that the solution of the flow equations for each hillslope and channel component must be independent of others in the network. The boundaries at the upslope divide, the base of the soil/rock profile and the vertical boundary beneath the mid point of the channel are assumed to be no-flow boundaries. The boundary segments immediately adjacent to the water filled channel are assumed to be fixed-head boundaries where, because of the requirement for independence, the water level in the channel is assumed fixed throughout the hillslope flow simulation. The vertical segment

of the Mth line of nodes that lies above the channel water level is assumed to be a seepage face boundary, with potentials fixed at atmospheric pressure if the soil is saturated and flow is towards the seepage face. Otherwise the unsaturated part of the potential seepage face is a no-flow boundary.

The top surface of the soil is a flux boundary with the fluxes controlled by the applied ground level input rates unless the surface becomes saturated and overland flow develops. The surface boundary then changes to a fixed head boundary while saturation persists, with the potentials fixed at atmospheric pressure. The errors involved here in neglecting a small depth of overland flow were felt to be negligible. The change of boundary conditions at the soil surface can occur locally on the slope so that the model can simulate the spread and contraction of a variable contributing area of overland flow. The upper boundary for the overland flow solution is always a zero flow boundary at a point marked by one of the nodes at the soil surface. The kinematic wave overland flow formulation does not require a lower boundary condition but will predict flows at the channel bank.

Further input data are required for each hillslope plane to describe the soil and root zone characteristics. Each layer of nodes is assigned to a particular soil type. Since the interpolation functions used in the finite element method ensure continuity of moisture potential at element boundaries, the soil hydraulic characteristics can vary arbitrarily between these soil horizons. Although the depths of each horizon may vary downslope it is currently assumed that the hydraulic characteristics of each layer or horizon do not change downslope. Each part of the soil surface is assigned to a particular vegetation type. Soil moisture characteristic parameters for each soil type and root zone characteristics for each vegetation type are input for the whole catchment at the start of a model run. The soil moisture characteristic parameters are described in section 4.2.3; the root zone characteristics required in section 4.2.4.

4.2.2 The finite element solution: the PHICAL, FORM and BANDED routines

In the finite element method equation 2 with its associated initial and boundary conditions is solved using the Galerkin method of weighted residuals. Zienkiewicz and Parekh (1970), Pinder and Frind (1972), Neuman (1973), Beven (1977, 1979a), Beven and Dunne (1982) and Yeh (1981) are examples of the application of the Galerkin method in subsurface hydrology. Pinder and Gray (1977) and Huyakorn and Pinder (1983) have provided useful reviews of the use of finite element methods in this field.

In the Galerkin method the continuous spatial variation of the dependent variable ϕ is approximated by a sum of products of basis functions $N_i(x,z)$ and the values $\phi_i(t)$ at the n nodal points of the finite element grid:

$$\hat{\phi} = \sum_{i=1}^{n} N_i(x,z)\ \phi_i(t)$$

where the basis functions N_i are chosen such that

$$N_i(x_j, z_j) = 1 \text{ when } i = j$$
$$= 0 \text{ when } i \neq j$$
and $N_i(x,z) \equiv 0$

outside the 'neighbourhood' of node i (i.e. the elements of which node i is a vertex).

If equation 2 is written in the form:

$$F(\phi) = 0$$

then

$$\iint_V WF(\phi)dV = 0$$

where W is some weighting function, is also true. Integrating by parts gives

$$\iint_V W\frac{\partial\phi}{\partial t}dV + \iint_V \left[\frac{\partial W}{\partial x}BK_x\frac{\partial\phi}{\partial x} + \frac{\partial W}{\partial z}BK_z\frac{\partial\phi}{\partial z}\right]dV \qquad (4)$$
$$- \int_S WK\nabla\phi.ndS = \iint_V [Q_s]WdV$$
$$= \hat{Q}_s, \text{ say,}$$

which is a weak form of equation 2, weakened by only being satisified in a weighted integral sense. This is approximated by putting $\phi=\Sigma N_j\phi_j$ and $W=N_i$ in turn to obtain

$$\iint_V \sum_{j=1}^{n} N_iN_jBC\frac{d\phi_j}{dt}dxdz$$

$$+ \iint_V \left\{\frac{\partial N_i}{\partial x}\sum_{j=1}^{n} BK_x\ \phi_j\frac{\partial N_j}{\partial x} + \frac{\partial N_i}{\partial z}\sum_{j=1}^{n} BK_z\ \phi_j\frac{\partial N_j}{\partial z}\right\}dxdz$$

$$+ \int_S \left\{N_i\sum_{j=1}^{n} BK_x\ \phi_j\frac{\partial N_j}{\partial x}l_x + N_i\sum_{j=1}^{n} BK_z\ \phi_j\frac{\partial N_j}{\partial z}l_z\right\}dS = \hat{Q}_s$$

where l_x and l_z are the local direction cosines of the outward normal to the domain boundary and the term involving ds represents an integral over the boundary and may be written $\int_S N_i\ B\ q\ dS$ where q is a boundary flux (positive inwards). In matrix form the resulting system of n equations corresponding to the n nodal points may be written as

$$G\phi + P\frac{d\phi}{dt} - F(t) = 0 \qquad (5)$$

where ϕ is the vector $\{\phi_i\}$, F(t) is the vector of boundary conditions including input and output, and remaining terms are $G=\{g_{ij}\}$, $P=\{p_{ij}\}$ where

$$g_{ij} = \int\int_V \left\{ BK_x \frac{\partial N_i}{\partial x}\frac{\partial N_j}{\partial x} + BK_z \frac{\partial N_i}{\partial z}\frac{\partial N_j}{\partial z} \right\} dxdz$$

$$p_{ij} = \int\int_V N_i N_j BC\, dxdz \qquad (6)$$

As an alternative to the use of a distributed capacitance matrix, P, as in equation 6, the IHDM offers the option of diagonally lumping this matrix. It is a matter of some debate which is the more hydrologically appropriate method and indeed whether a generalisation can be made on this point. Narasimham (1978), for example, presents a case for the lumped capacitance matrix being physically more realistic; Hromadka and Guymon (1980, 1981) suggest that the optimum degree of lumping may vary over time; and Frind and Verge (1978) suggest lumping is appropriate for unsaturated flow but not so for saturated problems.

Equation 5 contains a derivative with respect to time. In the IHDM the time derivative is represented by an implicit backward difference scheme as

$$G\Phi_{t+\Delta t} + \frac{P}{\Delta t}\left\{ \Phi_{t+\Delta t} - \Phi_t \right\} = \bar{F}$$

where $\bar{F}$ is an averaged value of F(t) over the time interval. It follows that

$$\left\{G + \frac{P}{\Delta t}\right\}\Phi_{t+\Delta t} = \bar{F} + \frac{P}{\Delta t}\Phi_t \qquad (7)$$

or $$A\Phi_{t+\Delta t} = H$$

Thus, given the values of ϕ at time t, the non-linear coefficents of the matrices are calculated at time $t+\Delta t$ where Δt is the time step. Previous work has shown that a backward difference time stepping technique has some advantage in maintaining stability in the solution of problems involving both saturated and unsaturated subsurface flow regions. The solution is iterative with the matrix coefficients at each iteration being calculated from the latest values of $\Phi_{t+\Delta t}$. The change in $\phi_{t+\Delta t}$ between each iteration is augmented by an acceleration factor w such that at the kth iteration

$$\phi^{\,k}_{t+\Delta t} = \phi^{\,k-1}_{t+\Delta t} + w\left[\phi^{\,k}_{t+\Delta t} - \phi^{\,k-1}_{t+\Delta t}\right]$$

The factor w is calculated dynamically at each iteration following the method of Cooley (1983).

In the IHDM the element integrations are based on linear interpolation functions for ϕ within quadrilateral elements. Subroutine PHICAL assembles the finite element matrix equations at each time step, calling on subroutine FORM to carry out the integrations for a single element. The element integrations are carried out using a Gauss point technique (see Pinder and Gray, 1977, and other finite element texts) with the non-linear coefficients evaluated from the interpolated values at every Gauss point. Up to 16 (4 by 4) Gauss points are currently allowed in each element (see figure 8). Gauss point integration has the advantage of giving a good representation of the change in the non-linear coefficients where hydraulic gradients are large, and where conditions change from saturated to unsaturated within an element. Very good mass balance is maintained by the solution compared with some other finite element techniques (see discussion in Yeh, 1981) because the balance is obtained by calculating the boundary fluxes directly from the finite element equations rather than from the predicted conductivity values and potential gradients close to the boundaries of the flow domain (see Lynch, 1984).

The matrix A in equation 7 is symmetric, which allows the matrix coefficients to be stored in a compact way as an N by MAX array where MAX is (b+1) where the total bandwidth of A is (2b+1). The complete set of equations is then solved in subroutine BANDED using a banded matrix solution algorithm derived from that of Zienkiewicz (1971).

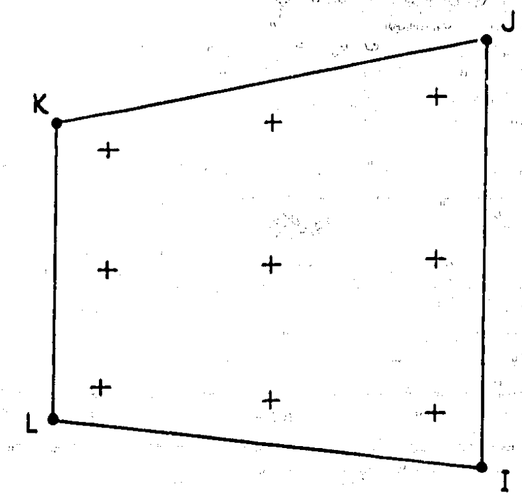

Fig. 8 Positions of 3 x 3 Gauss quadrature points in a quadrilateral element of arbitrary shape

4.2.3 The soil moisture characteristics: the CAPCON routine

Experience with numerical solutions of the Richards equation has suggested that the stability of finite difference and finite element solutions is improved if within the saturated zone the specific moisture capacity is small but non-zero. This implies some slight compressibility of the soil matrix with a resultant increase in porosity at potentials greater than zero. A further aid in maintaining stability is to ensure that the change in specific moisture capacity is smooth over the range of ψ values met during the simulation. Many functional representations of the soil moisture characteristic curves assume that there is a break in slope at the air entry potential or bubbling pressure of the soil (eg. Brooks and Corey, 1964; Campbell, 1974). In the IHDM a modification to the Campbell relationships has been used.

Thus, defining a relative potential p as ψ/ψ_o, where ψ_o is the air entry potential, the following relationships between ψ and θ are assumed to hold up to a relative potential of p_1.

For unsaturated moisture content:

$$\theta/\theta_s = p^{\alpha}$$

where θ_s is the saturated porosity of the soil and α is a constant. The specific moisture capacity is then given by

$$C(\psi) = \theta_s \alpha\, p^{\alpha-1}/\psi_o \qquad (8)$$

For unsaturated hydraulic conductivity:

$$K/K_s = p^{(-2+1\alpha)}$$

where K_s is the saturated hydraulic conductivity of the soil. This relationship for hydraulic conductivity is assumed to hold for all ψ values up to ψ_o, after which it takes on its saturated value.

At potentials between p_1 and 0, the moisture characteristic curve has been smoothed by assuming that:

$$\theta/\theta_s = 1 - \beta p - \gamma p^2$$

where β and γ are coefficients. The specific moisture capacity in this range is then given by

$$C(\psi) = -\theta_s \left(\beta + 2\gamma p\right)/\psi_o$$

At capillary potentials greater than 0

$$\theta/\theta_s = 1 - \beta p$$

with specific moisture capacity

$$C(\psi) = -\theta_s\, \beta/\psi_o \qquad (9)$$

The values of p_1 and γ can be chosen so that the specific moisture capacity is continuous with equation 8 at p_1, and continous with equation 9 at saturation. Using the data on the α and ψ_o parameter values for different soil textures given by Clapp and Hornberger (1978) and assuming some arbitrary values for the compressibility parameter β, values of γ and p_1 have been derived as shown in Table 2.

TABLE 2. Calculated soil moisture characteristic parameters for soils of different texture derived from data of Clapp and Hornberger (1978)

Soil type	α	β	γ	ψ_o (m)	p_1
sand	-0.247	0.001	0.0427	-0.121	1.60
loamy sand	-0.228	0.0005	0.0394	-0.090	1.61
sandy loam	-0.204	0.001	0.0351	-0.218	1.62
silt loam	-0.189	0.001	0.0325	-0.786	1.62
loam	-0.185	0.001	0.0319	-0.478	1.62
sandy clay loam	-0.140	0.001	0.0243	-0.299	1.63
silty clay loam	-0.129	0.001	0.0224	-0.356	1.63
clay loam	-0.117	0.001	0.0204	-0.630	1.64
sandy clay	-0.096	0.001	0.0166	-0.155	1.64
silty clay	-0.096	0.001	0.0166	-0.490	1.64
clay	-0.088	0.001	0.0152	-0.405	1.65

For explanation of variables see text

4.2.4 Evapotranspiration from the root zone: the EVAP routine

Negative ground surface fluxes output from the GLI preprogram indicate that there is some potential evapotranspiration demand remaining after losses from the interception storage have been satisfied. This residual evapotranspiration is distributed by the model between evaporation losses from surface flow and the

soil surface and transpiration from the root zone. If at any time step there is surface flow, then evaporation is assumed to take place from the surface water at the potential rate. If there is no overland flow then evapotranspiration from the soil is calculated on the basis of the potential rate, a root zone density distribution for the local vegetation type, and the local soil capillary potential. The relationship between the ratio of actual and potential evapotranspiration and capillary potential is based on the form used by Feddes et al., (1976a, b). This function has two parameters, the capillary potential, ψ_w, at wilting point and the capillary potential, ψ_s, at some anaerobiosis point at both of which actual evapotranspiration is assumed to fall to zero (figure 9).

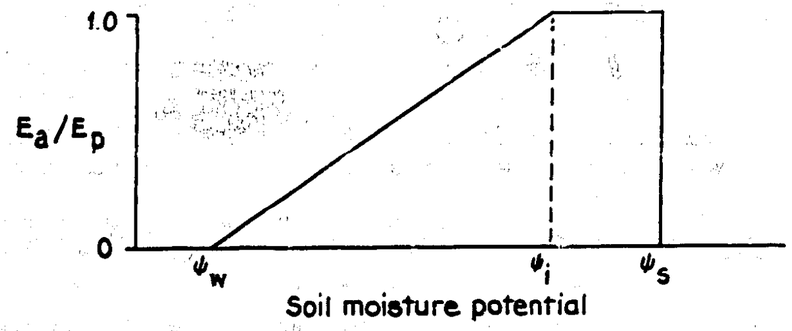

Fig. 9 Dependency of actual evapotranspiration E_a on potential evapotranspiration E_p and soil moisture potential (after Feddes et al., 1976a,b)

The reduction in actual evapotranspiration below the potential rate is calculated in subroutine EVAP using this function at every Gauss point in every finite element within the root zone on the hillslope. The actual evapotranspiration from each element is then weighted by the proportion of actively transpiring roots within the depth range covered by the element, as calculated from a root density function input to the model for each vegetation type. These proportions are calculated only once for each vegetation type on each hillslope plane (in subroutine PLANE) which implies that the depths of the nodes within the root zone should be identical for every vertical line of nodes on the slope. In practice this is not an important restriction. Each vertical line of elements may however be associated with a different vegetation type, with different root zone density functions, wilting point and anaerobiosis point parameters.

4.2.5 Kinematic overland flow: the FLOW and OVFLOW routines

Overland flow calculations are carried out whenever the soil surface reaches saturation. This may be due either to the input rate exceeding the calculated infiltration capacity of the soil, or due to saturation of the soil surface layer due to subsurface storage and flows. At the end of each subsurface time step, maximum infiltration rates at the soil surface are

calculated in subroutine PHICAL and these are used in subroutine FLOW to calculate net inputs to the overland flow solution for each surface boundary segment. A finer spatial discretisation than that provided by the surface nodes of the subsurface finite elements can be used, inputting a value for the maximum permissible spacing between overland flow solution nodes. Subroutine FLOW also calculates the net subsurface outflows from the seepage face and fixed head boundary segments of the hillslope, which form part of the discharges into the channel.

Since capillary potentials at the soil surface are set to zero (ie. equivalent to atmospheric pressure) if the surface becomes saturated, no account is taken of depths of overland flow in calculating infiltration rates and capacities. This simplifies the boundary calculations, helps maintain stability in both surface and subsurface solutions, and allows shorter time steps to be used in the surface flow solution where necessary.

Solution of the kinematic wave equation 3 requires specification of a single valued relationship between discharge and cross-sectional area of the flow. In the current model the relationship between Q and A is described by a power law function of the form

$$Q = fs^{0.5} A^b \qquad (10)$$

where s is the local slope angle and f is an effective roughness parameter, such that the kinematic wave velocity is given by $c = Qb/(Q/fs^{0.5})^{1/b}$. An effective depth of overland flow may be derived by dividing the area by the local slope width. The resulting equation is solved using a four point implicit finite difference scheme with discharge as the dependent variable, similar to that used by Li et al. (1975).

4.3 The channel calculations: the CHANEL routine

Channel routing in the IHDM has to deal with flows through a dendritic network of channels as specified in the network definition array. The equations for each channel component are solved sequentially, working downstream. This procedure requires that the channel sections be independent of the adjacent sections in the network (and independent of the hillslope planes which contribute headwater or lateral discharges). This will not be a restrictive assumption except in some long channels of low slope, where backwater effects may be expected to extend for considerable distances upstream.

The channel routine is based on the same kinematic wave equation and power law flow relationship as the overland flow solution on the hillslope planes, except that each channel section is assumed to be of uniform width. Subroutine CHANEL handles the input of the channel parameters, the setting up of initial conditions, the water balance calculations and the solution at each time step for a single channel component. Each channel passes a time sequence of discharges to the next channel downstream. Where a channel forms one arm of a junction in the network, discharges from both channels are added to form the upper boundary condition for the downstream channel.

The kinematic wave solution for the channel elements uses the same implicit solution algorithm as for the overland flow case. This has been programmed so that it is very easy to incorporate discharge/cross-sectional area flow relationships other than the power law of equation 10 simply by changing the calculation of the wave speeds. Beven (1979b) for example has suggested a relationship for steep upland channels of the form

$$Q = a\,(A - A_o)$$

where A_o is the minimum cross-sectional area below which there is no flow. This has a constant wave speed, $c = dQ/dA = a$, and results in a linear routing algorithm. This and other single valued flow relationships are easily incorporated into the solution.

The initial conditions in each channel section are either read from a file produced by a previous run, or are calculated from initial downstream and upstream discharges input to the model. Where these differ, a uniform lateral inflow or loss is assumed along the channel in calculating the initial flows at each node. The kinematic wave solution takes as its upper boundary condition the known values of discharge given by the flows from an upstream channel, junction of channels, or headwater hillslope plane. At each time step, the equations are solved node by node working downstream. No lower boundary condition is required.

4.4 Other subroutines of the IHDM

There are three additional subroutines in IHDM that have not been mentioned in the preceding discussion. Subroutine STORE is used to calculate the total volumes of water stored in the subsurface flow domain at the beginning and end of a simulation for use in the water balance check calculations.

Subroutine LNPLOT gives a simple lineprinter plot of discharges from any chosen hillslope or channel component and will also plot observed discharge data if they are available.

Subroutine GRAPH is used to provide various levels of data printout to a file or lineprinter for the hillslope planes during a simulation depending on the input value of a control variable. At the most detailed level of output, all the elements of the finite element matrices at every iteration may be printed. At a lesser level, values of capillary potential and hydraulic potential for all the subsurface nodes and discharges for the surface flows are printed out. If this routine is not called at all, only a summary output is given at the end of each time step.

4.5 Additional features of IHDM: the restart options

The current implementation of the IHDM allows the simulation to be restarted after any completed hillslope or channel component. When the calculations for a given component are complete, the values of the solution

variable (hydraulic potential for subsurface flows, discharges for surface flows) are written to a file. The time sequence of discharges produced by each element is also written to a file. The solution may then be restarted in one of two ways. If the simulation has been satisfactory for all the hillslope and channel components the final values of the solution variables may be read as the initial conditions for a subsequent period. Alternatively, if it is desired to change the parameter values or time steps for a hillslope or channel element to examine the effect on the predicted flows for the current simulation, then that simulation can be restarted immediately before the component for which changes have been made, avoiding unnecessary recalculations for previous components.

5. Example simulations

As a demonstration of the simulations produced by the hillslope component of the IHDM, the model has been used here to predict the hydrological response of a particular hillslope form, based on the Wye catchment at Plynlimon, to a single 56 mm 18 hour rainstorm for different combinations of parameter values and initial conditions. The soil was assumed to have a constant depth of 1.0 m all over the 640 m length slope. A finite element mesh defined by 14 vertical lines of 10 nodes at depths of 0, 0.02, 0.05, 0.1, 0.2, 0.3, 0.4, 0.6, 0.8 and 1.0 m was used, giving a total of 117 elements in all. A summary of the simulation runs carried out is given in table 3. All these runs produced slope discharge which was a combination, in differing proportions, of throughflow and overland flow, the latter being of both infiltration excess and saturation excess origin.

Figure 10a shows unit width slope discharges for three simulations differing only in terms of the (spatially constant) initial moisture potential. The increasingly wetter initial conditons are seen to promote higher and earlier peak runoff in association with higher proportions of overland flow (table 3).

In figure 10b model runs differing only in terms of saturated hydraulic conductivity values are compared. Lower conductivities are associated with greater amounts and proportions of overland flow, through their influence on effective infiltration capacity. Where, in the case of the highest conductivity used, flow is predominantly subsurface, the effect of a high conductivity in raising baseflow and reducing time to peak is apparent.

Figure 10c shows an example of the effect of contour curvature on hillslope discharge, maintaining slope profile form, drainage area and all other aspects of the model constant. The convergent slope promotes early saturation and a downslope concentration of overland flow, contributing to a greatly increased peak compared with the straight-contour slope. The divergent slope to some extent disperses flow compared to the straight slope, showing a greater proportion of throughflow and, for this hydraulic conductivity, a slightly later peak.

TABLE 3. Summary of Wye hillslope simulations

S = straight contour slope, D = divergent slope (1:10), C = convergent slope (10:1); TF = throughflow (remainder of slope discharge being overland flow)

run	slope	K_x, K_z m hr^{-1}	initial moisture potential m	peak flow m^3 hr^{-1} m^{-1}	TF %
1	S	0.72	-0.15	3.76	22
2	S	0.72	-0.10	4.42	17
3	S	0.72	-0.20	1.80	35
4	S	0.072	-0.15	4.19	3
5	S	7.20	-0.15	2.62	80
6	C	0.72	-0.15	20.80	5
7	D	0.72	-0.15	1.96	36

Fig. 10 IHDM4 simulations of hillslope discharge. For run details see Table 3

a) effects of initial conditions

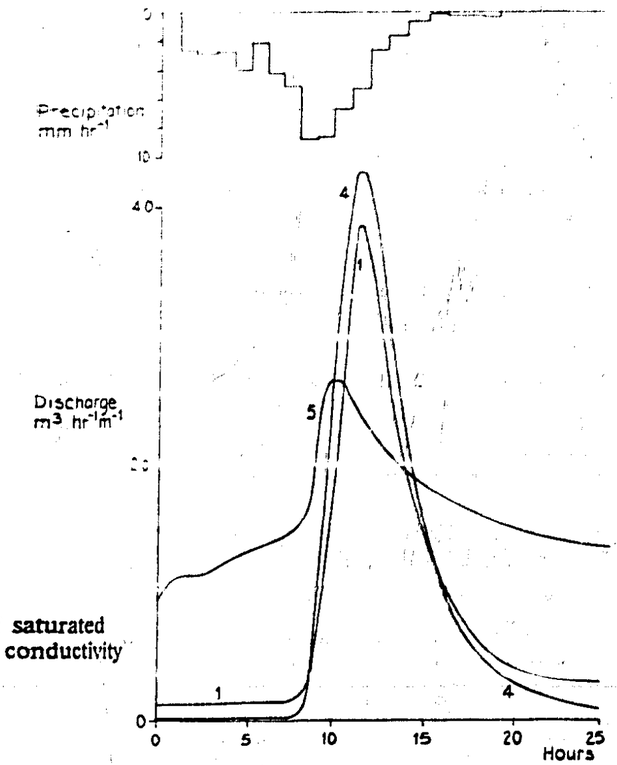

b) effects of saturated hydraulic conductivity values

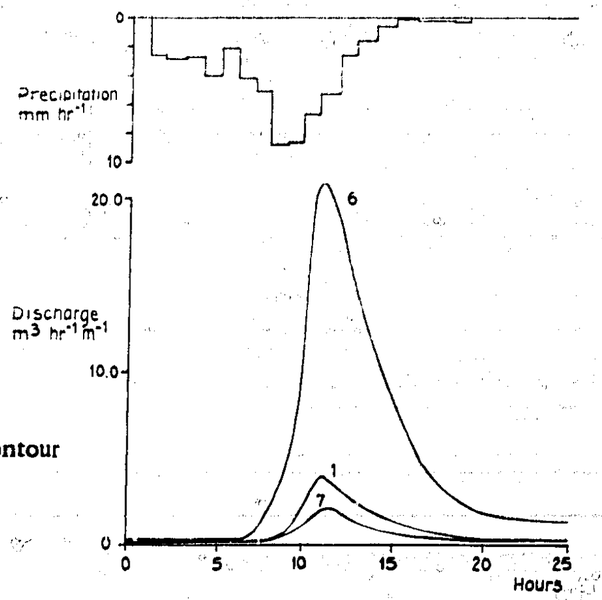

c) effects of contour curvature

6. Model calibration

The parameters of physically-based models are in principle measurable in the field: experiments could be carried out to determine values of hydraulic conductivity, porosity, overland flow roughness, interception capacity, and the other parameters required, as summarised in table 4. In practice an application of a physically-based model is rarely associated with a complete measurement programme, since field measurements are both time-consuming and labour intensive, particularly where, as in catchment hydrology, it is known that parameter values vary in space so that a number of measurements will be required to characterise the system.

TABLE 4. Table of physical parameters required by the IHDM

For each input zone:

Z_o	Aerodynamic roughness height of snow (or degree-day factor)
R_s	Density of snow
$\alpha_1\alpha_2\alpha_3$	Albedo parameters for snow
HVEG	Height of vegetation canopy
ZPD	Zero plane displacement height of vegetation
ZET	Aerodynamic roughness height of vegetation
CMAX	Interception storage capacity of vegetation
RUTK,RUTB	Parameters of Rutter interception drainage function
CAI	Leaf area index
PLAI	Proportion of ground surface covered by vegetation

For each soil type:

SKX	Horizontal saturated hydraulic conductivity
SKZ	Vertical saturated hydraulic conductivity
THS	Porosity
SA,SB,SC	Parameters of soil moisture characteristic
PSIO,PSI	functions (see section 4.2.3)

For each root zone type:

DEPTH( )	Array of depths
RDF( )	Array of equivalent cumulative proportions of active roots
ETPSIW	Wilting point potential
ETPSIL	Anaerobiosis point potential

For overland flow on each hillslope:

BOF	Power in overland flow function (equation 21)
OFC	Roughness parameter in overland flow function.

For each channel segment:

BCH	Power in channel flow function
CHC	Roughness parameter in channel flow function

This spatial variability poses interesting problems for the application of physically-based models. On the one hand, if that variability were known then the distributed nature of such models would allow it to be taken into account. On the other hand, making sufficient measurements to properly assess the variability in the many parameters required by these models would be an extremely expensive exercise. In addition, there is a problem of scale that must be considered. Many measurement techniques, particularly for soil properties and variables, involve sampling at only very small scales. Distributed models commonly use grid or element scales that average soil properties over metres or tens of metres. The parameter values appropriate at the model grid scale may not show the same variability as that evident at the measurement scale, particularly when the integrative nature of downslope flow processes is taken into account. It may then be the case that, at the model grid scale, a set of spatially uniform 'effective' parameter values provide satisfactory simulations. Most applications of physically-based models that have been published to date have assumed that 'effective' parameter values can be used at least for each soil horizon or vegetation type. These effective parameters have generally been determined by trial and error calibration, usually from a starting point constrained by measurements or *a priori* estimation of parameters on the basis of the physical characteristics of the catchment. There have been a few studies that have suggested empirical relationships between the type of parameters required by physically-based models and more readily available characteristics. Clapp and Hornberger (1978) and McCuen et al. (1981), for example, provide relationships between parameters of the soil moisture characteristic curve and soil texture, and Betson (1979) has related channel routing parameters to basin characteristics.

Trial and error calibration presupposes some measurements of system performance with which the simulated behaviour may be compared. Parameters (and initial conditions) are changed in turn until a 'best fit' simulation is obtained that matches the observed behaviour as closely as possible. Although there are automatic methods available for the calibration of models they have not to date been used with distributed physically-based models because of the computational expense that would be involved. However the use of such methods with simpler models has revealed a number of problems that may, by analogy, also hold for the calibration of physically-based models. In particular it has been found that given a large number of parameters it is almost always possible to obtain a reasonable fit to the relatively simple trace of the integrated system response that is the hydrograph, and moreover to do so with combination of parameter values that are not the 'true' values for the catchment. Insensitive parameters, and parameters that are intercorrelated in their effect on the simulated hydrograph may make calibration by fitting particularly difficult (see, for example, Ibbitt and O'Donnell, 1971, Sorooshian and Gupta, 1983, Hornberger et al., 1985). Applications of version 3 (Rogers et al., 1985) and version 4 of the IHDM (Calver, in press) to the Tanllwyth catchment suggest the most sensitive parameters of the model under this hydrological regime are the saturated hydraulic conductivity and the overland flow roughness.

One potential advantage of physically-based models in this respect is that, given knowledge of the physical characteristics of a catchment, the possible range of values that are considered in calibration can be constrained. This advantage

may in cases prove difficult to apply because of the approximations in the way the model represents reality. In assessing the saturated hydraulic conductivity of a soil of a particular texture, for example, it can be important (but currently very difficult) to take account of the macroporosity of the soil. Similarly, in assessing overland flow parameters it may be important to take account of the effect of the many pipes, rills, gullies, ditches and small ephemeral channels that are important in the surface flow process but which cannot be accurately represented at the scale of the model hillslope components.

A second advantage of physically-based models in calibration is that they produce not only estimates of catchment discharges but also predictions of internal state variables such as soil moisture and water table levels, and where there are measurements of such variables they can be taken into account in the calibration process. Very few catchment studies have compared model results with measurements of internal state variables, and with only limited success (see, for example, Stephenson and Freeze, 1974). IHDM4 predictions of soil moisture and process status during the course of a calibrated Tanllwyth storm hydrograph were investigated (Calver, in press) and, though no quantitative data exist for direct comparison, the simulated conditions accorded reasonably well with qualitative field experience.

Stephenson and Freeze (1974) point out that having calibrated a physically-based distributed model, validating it by further simulations also poses difficulties. An ideal validation presupposes perfect knowledge of the initial and boundary conditions, something that is never attainable in practice. Estimation of those boundary conditions also introduces flexibility into the simulation of any validation period.

Procedures for calibrating physically-based models such as the IHDM remain therefore the subject of research. We can expect that, although it is possible to calibrate by comparison with observed behaviour, or estimate parameter values from physical reasoning, or use whatever field measurements are available, there will always be some uncertainty associated with the parameter values however they are obtained. A relatively simple way of estimating the uncertainty in the simulated variables that arises from uncertainty in the parameter values has been applied to the IHDM3 (Rogers et al., 1985).

Whilst recognising these possible limitations, it has nevertheless been considered worthwhile to use calibrated values of soil properties (hydraulic conductivity, porosity, surface roughness) for a winter Tanllwyth storm on temporal and spatial transposition studies (Calver, in press). Confidence in the calibrated parameter set was enhanced by successful predictions for other winter runoff events in the Tanllwyth (see, for example, figure 11a). Further, such soil parameter values were used on a similar adjacent catchment, the Hore, and, with precipitation and topographic data files constructed specifically for the latter, gave encouraging flow predictions (figure 11b). Such an exercise is, of course, a necessary prerequiste to any possibilities of the use of the model in catchments where little monitoring is undertaken.

It is anticipated that further work will better define the uncertainties associated with model predictions and provide some practical guidelines for its use. The IHDM offers the potential for investigating aspects of physical hydrology

outside the range for which field experiments are in practice easily devised, and as such may enhance our knowledge of process behaviour and extend data sets for use with other techniques of hydrological analysis. In summary, it is hoped that the IHDM will provide a general and flexible package for physically-based catchment modelling.

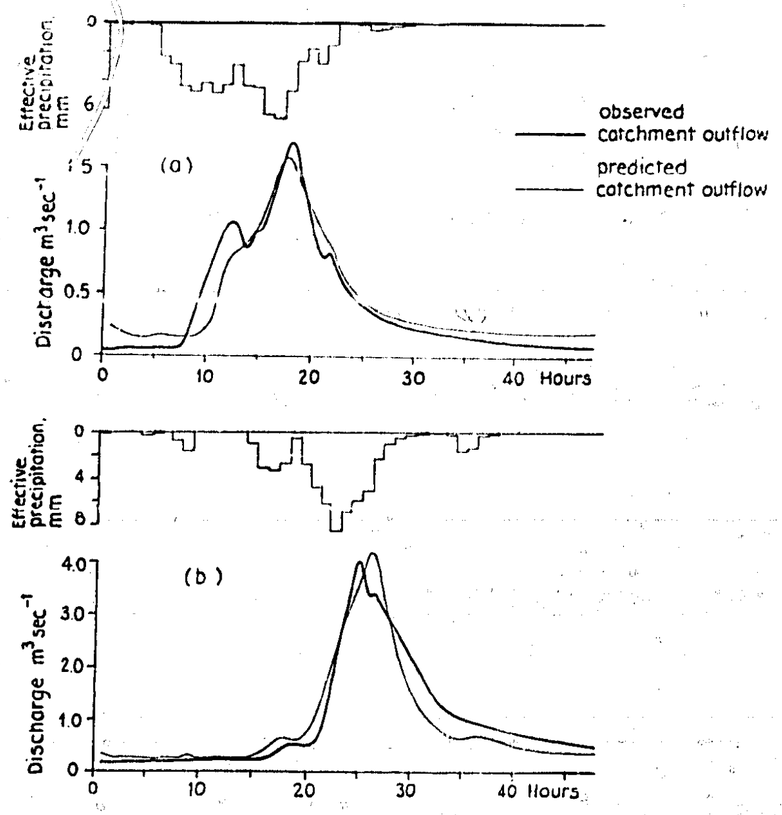

Fig. 11 IHDM4 simulations using calibrated soil parameters for Tanllwyth storm of 19 November 1977 on
a) storm of 12 February 1976 in Tanllwyth
b) storm of 19 November 1977 in Hore catchment
(after Calver, in press)

Acknowledgements

The authors are grateful to all those who have helped to develop and test the IHDM models, in particular to A. Binley, D.M. Cooper, J. Daluz Vieira, R. Harding, C. Rogers, W.L. Wood and D. Woolhiser.

References

Abbott, M.B., Bathurst, J.C., Cunge, J.A., O'Connell, P.E., and Rasmussen, J., 1986a. An introduction to the European Hydrological System - Système Hydrologique Européen, 'SHE'. 1. History and philosophy of a physically-based, distributed modelling system. Journal of Hydrology, 87, 45-59.

Abbott, M.B., Bathurst, J.C., Cunge, J.A., O'Connell, P.E. and Rasmussen, J., 1986b. An introduction to the European Hydrological System - Système Hydrologique Européen, 'SHE'. 2. Structure of a physically-based, distributed modelling system. Journal of Hydrology, 87, 61-77.

Bathurst, J.C., 1986. Physically-based modelling of an upland catchment using the Système Hydrologique Européen. Journal of Hydrology, 87, 79-102.

Bear, J., 1972. Dynamics of fluids in porous media. Elsevier.

Betson, R.P., 1979. A geomorphic model for use in streamflow routing. Water Resources Research, 15, 95-101.

Beven, K.J., 1977. Hillslope hydrographs by the finite element method. Earth Surface Processes, 2, 13-28.

Beven, K.J., 1979a. Experiments with a finite element model of hillslope hydrology: the effect of topography. In Surface and Subsurface Hydrology, Proceedings of the third international hydrology symposium, Fort Collins, Colorado.

Beven, K.J., 1979b. On the generalized kinematic routing method. Water Resources Research, 15, 1238-1242.

Beven, K.J., 1985. Distributed models. In M.G. Anderson and T.P.Burt (eds): Hydrological Forecasting, 405-435, Wiley.

Beven, K.J. and Dunne, T., 1982. Modelling the effect of runoff processes on snowmelt hydrographs. In V.P.Singh (ed): Rainfall-runoff relationship. Water Resource Publications, Littleton, Colorado.

Beven, K.J. and O'Connell, P.E., 1982. On the role of physically-based distributed modelling in hydrology. Institute of Hydrology Report 81, Wallingford, UK.

Beven, K.J., Warren, R. and Zaoui, J., 1980. SHE: Towards a methodology for physically-based distributed forecasting in hydrology. In Hydrological Forecasting. IAHS Publication 129, 133-137.

Brooks, R.H. and Corey, A.T., 1964. Hydraulic properties of porous media. Hydrology paper No.3, Colorado State University, Fort Collins, Colorado, 1964.

Calver, A. in press. Calibration, sensitivity and validation of a physically-based rainfall-runoff model. Journal of Hydrology.

Campbell, G.S., 1974. A simple method for determining unsaturated conductivity from moisture retention data. Soil Science, 117, 311-314.

Clapp, R.B. and Hornberger, G.M., 1978. Empirical equations for some soil hydraulic properties. Water Resources Research, 14, 601-604.

Cooley, R.L., 1983. Some new procedures for numerical solution of variably saturated flow problems. Water Resources Research, 19, 1271-1285.

Daluz Vieira, J.H., 1983. Conditions governing the use of approximations for the Saint-Venant equations for shallow surface water flow. Journal of Hydrology, 60, 43-58.

Engman, E.T. and Rogowski, A.S., 1974. A partial area model for storm flow synthesis. Water Resources Research, 10, 464-472.

Feddes, R.A., Kowalik, P., Kolinska-Malinka, K. and Zaradny, H., 1976a. Simulation of field water uptake by plants using a soil water dependent root extraction function. Journal of Hydrology, 31, 13-26.

Feddes, R.A., Kowalik, P., Neuman, S.P. and Bresler, E., 1976b. Finite difference and finite element simulation of field water uptake by plants. Hydrological Sciencies Bulletin, 21, 81-98.

Freeze, R.A., 1971. Three-dimensional, transient, saturated-unsaturated flow in groundwater basin. Water Resources Research, 7, 347-366.

Freeze, R.A., 1972a. Role of subsurface flow in generating surface runoff. 1. Base flow contributions to channel flow. Water Resources Research, 8, 609-623.

Freeze, R.A., 1972b. Role of subsurface flow in generating surface runoff. 2. Upstream source areas. Water Resources Research, 8, 1272-1283.

Freeze, R.A., 1978. Mathematical models of hillslope hydrology. In M.J. Kirkby, (ed): Hillslope Hydrology, 177-225. Wiley

Freeze, R.A. and Harlan, R.L., 1969. Blueprint for a physically-based, digitally-simulated hydrologic response model. Journal of Hydrology, 9, 237-258.

Frind, O.E. and Verge, M.J., 1978. Three-dimensional modelling of groundwater flow systems. Water Resources Research, 14, 844-856.

Hornberger, G.M., Beven, K.J., Cosby, B.J. and Sappington, D.E., 1985. Shenandoah Watershed Study: calibration of a topography-based, variable contributing area model to a small forested catchment. Water Resources Research, 21, 1841-1850.

Hromadka, T.V. and Guymon, G.L., 1980. Some effects of linearizing the unsaturated soil moisture transfer diffusivity model. Water Resources Research, 16, 643-650.

Hromadka, T.V. and Guymon, G.L., 1981. Improved linear trial function finite element model of soil moisture transport. Water Resources Research, 17, 504-512.

Huyakorn, P.S. and Pinder, G.F., 1983. Computational methods in subsurface flow. Academic Press, N.Y.

Ibbitt, R.P. and O'Donnell, T., 1971. Fitting methods for conceptual catchment models. Journal of the Hydraulics Division, American Society of Civil Engineers, 97, 1331-1342.

Li, R.M., Simons, D.B. and Stevens, M.A., 1975. Nonlinear kinematic wave approximation for water routing. Water Resources Research, 11, 245-252.

Lynch, D.R., 1984. Mass conservation in finite element groundwater models. Advances in Water Resources, 7, 67-75.

McCuen, R.H., Rawls, W.J. and Brakensiek, D.L., 1981. Statistical analysis of the Brooks-Corey and Green-Ampt parameters across soil textures. Water Resources Research, 17, 1005-1013.

Morris, E.M., 1980. Forecasting flood flows in grassy and forested basins using a deterministic distributed mathematical model. In Hydrological Forecasting. IAHS Publication 129, 247-255.

Morris, E.M., Blyth, K. and Clarke, R.T., 1980. Watershed and river channel characteristics and their use in a mathematical model to predict flood hydrographs. In G. Fraysse (ed): Remote sensing application in agriculture and hydrology. Balkema, Rotterdam, 431-446.

Morris, E.M. and Woolhiser, D.A., 1980. Unsteady one-dimensional flow over a plane: partial equilibrium and recession hydrographs. Water Resources Research, 16, 355-360.

Narasimhan, T.N., 1978. A perspective on numerical analysis of the diffusion equation. Advances in Water Resources, 1, 147-155.

Neuman, S.P., 1973. Saturated-unsaturated seepage by finite elements. Journal of the Hydraulics Division, American Society of Civil Engineers, 99, 2233-2250.

Pinder, G.F. and Frind, E.O., 1972. Application of Galerkin's procedure to aquifer analysis. Water Resources Research, 8, 108-120.

Pinder, G.F. and Gray, W.G., 1977. Finite element simulation in surface and subsurface hydrology. Academic Press, New York.

Richards, L.A., 1931. Capillary conduction of liquids through porous mediums. Physics, 1, 318-333.

Rogers, C.C.M., Beven, K.J., Morris, E.M. and Anderson, M.G., 1985. Sensitivity analysis, calibration and predictive uncertainty of the Institute of Hydrology Distributed model. Journal of Hydrology, 81, 179-191.

Ross, B.B., Contractor, D.D. and Shanholtz, V.O., 1979. A finite-element model of overland and channel flow for assessing the hydrologic impact of land-use change. Journal of Hydrology, 41, 11-30.

Smith, R.E. and Woolhiser, D.A., 1971. Overland flow on an infiltrating surface. Water Resources Research, 7, 899-913.

Sorooshian, S. and Gupta, V.K., 1983. Automatic calibration of conceptual rainfall-runoff models; the question of parameter observability and uniqueness. Water Resources Research, 19, 260-268.

Stephenson, G.R. and Freeze, R.A., 1974. Mathematical simulation of subsurface flow contributions to snowmelt runoff, Reynolds Creek watershed, Idaho. Water Resources Research, 10, 284-294.

Weinstock, R., 1952. Calculus of variations. McGraw-Hill, NY.

Woolhiser, D.A. and Liggett, J.A., 1967. Unsteady, one-dimensional flow over a plane - the rising hydrograph. Water Resources Research, 3, 753-771.

Yeh, G-T., 1981. On the computation of Darcian velocity and mass balance in the finite element modeling of groundwater flow. Water Resources Research, 17, 1529-1534.

Zienkiewicz, O.C., 1971. The finite element method in engineering. McGraw Hill.

Zienkiewicz, O.C. and Parekh, C.J., 1970. Transient field problems: two-dimensional and three-dimensional problems by iso-parametric finite elements. International Journal for Numerical Methods in Engineering, 2, 61-71.